JOURNAL OF MECHANICS OF MATERIALS AND STRUCTURES
Vol. , No. ,

A MARCHING PROCEDURE FOR FORM-FINDING FOR TENSEGRITY STRUCTURES

ANDREA MICHELETTI AND WILLIAM O. WILLIAMS

We give an algorithm for solving the *form-finding* problem, that is, for finding stable placements of a given tensegrity structure. The method starts with a known stable placement and alters edge lengths in a way that preserves the equilibrium equations. We then characterize the manifold to which classical tensegrity systems belong, which gives insight into the form-finding process. After describing several special cases, we show the results of a successful test of our algorithm on a large system.

1. Introduction

Tensegrity structures, popularized by Buckminster Fuller following sculptures by Kenneth Snelson, have become familiar to most structural engineers and architects through their applications, in particular, to lightweight domes and to decorative structures [Pellegrino 1992; Snelson 1996]. These structures consist of a combination of rigid bars, which carry tension or compression, and inextensible cables, which can carry no compression. Pin joints connect the elements at their ends.[1] The engineering studies of trusses by Möbius and Maxwell, as well as Cauchy's analysis of the rigidity of polygonal frames, only considered traditional pinned-bar structures [Cauchy 1813; Möbius 1837; Maxwell 1869]. Calladine and Pellegrino (in the engineering literature) and Roth et al. (in the mathematical literature) extended these results to tensegrity structures [Calladine 1978; Pellegrino and Calladine 1986; Calladine and Pellegrino 1991; Roth and Whiteley 1981]. Extensive bibliographies and more recent results appear in [Connelly and Whiteley 1996; Skelton et al. 2001; Motro 2003; Williams 2003; Tibert and Pellegrino 2003; Masic et al. 2006; So and Ye 2006].

We are interested in the *form-finding problem*: given the graph of a structure, along with the relative positions of crossing elements if the graph is not planar, find which physical placements in space will result in a stable structure. Several methods which have been used to attack the form-finding problem are outlined in [Tibert and Pellegrino 2003]. Motro [1984] employed dynamic relaxation, an algorithm first introduced in [Day 1965], which has been reliably applied to tensile structures [Barnes 1999] and many other nonlinear problems. Pellegrino [1986] formulated an equivalent constrained minimization problem, and, since 1994, Burkhardt has been making extensive use of techniques from nonlinear programming [2005]. Connelly and Back [1998] applied group representation theory to discover numerous symmetric placements. Vassart and Motro [1999] employed the force density method, which was first introduced

Keywords: tensegrity structures, stability analysis, rank-deficiency manifold, marching processes, limit placements.
The research presented in this paper was partly conducted during Micheletti's 2004 visit to the Department of Mathematical Sciences of Carnegie Mellon University. Financial support from the Center of Nonlinear Analysis is gratefully acknowledged.

[1] Without essential change in the computations, one may also introduce elements called *struts*, which are unpinned bars that admit no tension. We do not consider struts, as they are of less practical interest.

in [Linkwitz and Schek 1971] for form-finding of tensile structures, according to Schek [1974]. Skelton et al. [2002] presented an algebraic approach specialized to structures with noncontiguous bars, and Paul et al. [2005b] used genetic algorithms. Most recently, Zhang and Ohsaki [2005] and Estrada et al. [2006] developed new numerical methods using a force density formulation, and Zhang et al. [2006] employed a refined dynamic relaxation procedure.

The form-finding problem has no complete solution, although many authors have examined sufficient conditions. The most convenient sufficient condition, which we use here, is the second-order stress test. This test is stronger than the minimal-energy condition, but equivalent to it in most common situations. More precisely, it is not a necessary condition for stability, since there can be stable structures for which it is not satisfied, but it is a necessary and sufficient condition in order to have a structure possessing first-order positive stiffness. Since we model bars as rigid and cables as inextensible, local or global buckling instabilities must be considered separately, depending on the material properties of the elements in the structure; see [Ohsaki and Zhang 2006].

Unfortunately, the known stability conditions, including the second-order test, are descriptive rather than prescriptive. That is, they are easily applied to test a given placement of the structure, but are difficult to exploit for the discovery of exact or approximate stable placements. We propose, instead, a practical algorithm for the form-finding problem which is based on setting up a system of differential equations. This system can be solved numerically to obtain a family of stable placements. The trajectory of these solutions must start at a stable placement, so the process requires we have a beginning point which is a stable structure. However, the literature offers many examples of such placements; see, for example, [Nishimura 2000; Murakami and Nishimura 2001; Sultan et al. 2001; Micheletti 2003]. Often, their high degree of symmetry enables analytic construction.

Our method has practical relevance in all those applications in the lengths of elements are changed continuously in order to pass from one configuration to another. This includes foldable, deployable, or variable-geometry structures. Furuya [1992] and Hanaor [1993] pioneered the analysis and design of tensegrity structures with these characteristics. More recent studies include [Oppenheim and Williams 1997; Bouderbala and Motro 1998; Sultan and Skelton 1998; Tibert 2002; Aldrich et al. 2003; Defossez 2003; El Smaili et al. 2004; Fest et al. 2004; Paul et al. 2005a; Schenk et al. 2007].

Here is an outline of our paper. After introducing notation and concepts in Section 2, we summarize some general results on tensegrity structures in Section 3. Most of these results are scattered throughout the mathematical and engineering literature, so a coherent summary facilitates discussion of the use and limitations of the form-finding process. We also present several example structures that illustrate the limitations of these results. In Section 4, we characterize the sets of placements to which our method applies: the rank-deficient manifolds. We briefly illustrate singular cases within the characterization. Finally, in Section 5, we describe our algorithm, and give examples of its application.

2. Structural analysis of trusses

Figure 1 shows an example of a truss (we give examples in two dimensions, to keep the diagrams simple). Trusses have a graph structure in which the edges are bars, and the nodes are the pin joints which connect the bars. The symbol $\boldsymbol{A}$ denotes the *structural matrix*, also known as the *equilibrium matrix*. The vector $\mathbb{f}$ of externally applied forces is indexed by the nodes of the structure, and the vector $\boldsymbol{\tau}$ of forces in the

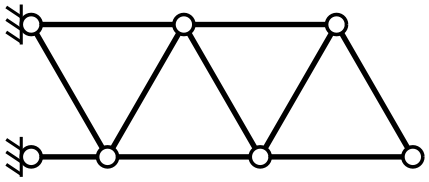

Figure 1. A simple two-dimensional truss.

edges of the structure is indexed by edge. There is a linear relationship between these two vectors:

$$\mathbb{f} = \boldsymbol{A}\boldsymbol{\tau}. \tag{1}$$

Dual to this is the relation between $\mathbb{v}$, the vector of node velocities (or, in engineering terms, infinitesimal motions), and $\boldsymbol{\delta}$, the vector of rates of change of the edge lengths:

$$\boldsymbol{\delta} = \boldsymbol{A}^T \mathbb{v}. \tag{2}$$

We will consider a variant of this model which is more convenient for calculations. Consider a structure in three dimensions, with n pins, located at the placement

$$\mathbb{p} := (\boldsymbol{p}_1, \ldots, \boldsymbol{p}_n), \quad \boldsymbol{p}_r \in \mathbb{R}^3. \tag{3}$$

An edge is notated by its set of end nodes: $\{ij\}$. Let E be the set of all k edges in the structure. Next, we construct the so-called *geometric matrix* Π by specifying its column vectors, one per edge:

$$\boldsymbol{\pi}_{ij}(\mathbb{p}) = \begin{bmatrix} \mathbf{0} \\ \vdots \\ \mathbf{0} \\ \boldsymbol{p}_i - \boldsymbol{p}_j \\ \mathbf{0} \\ \vdots \\ \mathbf{0} \\ \boldsymbol{p}_j - \boldsymbol{p}_i \\ \mathbf{0} \\ \vdots \\ \mathbf{0} \end{bmatrix} \in \mathbb{R}^{3n}. \tag{4}$$

Here the entries, indexed by the list of nodes, are values in $\mathbb{R}^3$. The nonzero entries in (4) are in the i-th and j-th rows, respectively. To change this matrix into the corresponding equilibrium matrix $\boldsymbol{A}$, one divides each column vector $\boldsymbol{\pi}_{ij}$ by the length of the corresponding edge.

Using this formulation, the balance of forces at each node is expressed as

$$\mathbb{f} = \Pi\boldsymbol{\omega}, \tag{5}$$

in which $\mathbb{f}$ is the force vector of external forces applied to the nodes, and the *stress vector* $\boldsymbol{\omega}$ for the placement is a vector in $\mathbb{R}^k$ whose ij entry is the scalar force in the edge ij divided by the length of

the edge.[2] Physically, one pictures an applied set of nodal forces generating stresses in the structure to support them. If the structure is redundant (has an "excess" number of edges), it may admit a self-equilibrating stress or *self stress* $\boldsymbol{\omega}$ satisfying

$$\Pi\boldsymbol{\omega} = \mathbf{0}. \tag{6}$$

Next, we turn to kinematics. We consider a velocity $\mathbb{v}$, as before. Then Π associates to $\mathbb{v}$ a rate of change of the length of each edge in the structure, which is given by

$$\boldsymbol{\epsilon} = \Pi^T \mathbb{v}, \quad \text{or} \quad \epsilon_{ij} = \boldsymbol{\pi}_{ij} \cdot \mathbb{v} = (\boldsymbol{p}_i - \boldsymbol{p}_j) \cdot (\boldsymbol{v}_i - \boldsymbol{v}_j), \tag{7}$$

in which ϵ_{ij} is the rate of change of the length of edge ij, times the length of the edge. Physically, we picture a velocity imposed on each node, which lengthens or shortens the edges.

We choose to consider only *constrained* structures, that is, structures in which several nodes are fixed to the earth. This means that these nodes only admit zero velocities. Also, we only consider cases in which enough nodes are fixed that there can be no rigid-body motions of the entire structure.[3] For such a structure, a velocity which leaves all edge lengths unchanged is a flexibility in the structure. If $\mathbb{v} \neq 0$ and

$$\Pi^T \mathbb{v} = \mathbf{0}, \tag{8}$$

we call $\mathbb{v}$ a flexure or a *mechanism.*

The nullspace of Π is the set of all self stresses. This space is a subspace of $\mathbb{R}^k$. We call its dimension s the *number of self stresses.* Likewise, we call the dimension m of the nullspace of Π^T the *number of mechanisms.*

Finally, we discuss stability. A *motion* of a structure is a time-parameterized family of placements $\mathbb{q}(t)$. The time derivative at $t = 0$, $\dot{\mathbb{q}}(0)$, is a velocity for the placement $\mathbb{p} = \mathbb{q}(0)$. An *admissible* motion of the structure leaves edge lengths unchanged. Since our assumptions rule out rigid-body motions, any admissible motion represents a mode of collapse of the structure. The initial velocity of a collapsing motion is a mechanism, and hence one can avoid collapse by ensuring that no mechanisms occur. However, the existence of a mechanism does not imply that there is a collapsing motion.

Our nomenclature reflects the distinction between these two possibilities. A placement of the structure is said to be *stable* if admits no admissible motions away from that placement, and the structure is said to be *rigid* in that placement if it admits no mechanisms.[4] Thus, rigidity implies stability, but the converse is false, in general. The converse may be true in specific cases: Asimow and Roth [1979] show that it holds if the present placement produces a local maximum in rank for the geometric matrix.

3. Tensegrity structures

Figure 2 shows an example of a tensegrity structure. These structures have a more restrictive definition than arbitrary trusses. First, the stress in a cable edge must be nonnegative (that is, a tension). We call a

[2] The literature often refers to ω_{ij} as the *force density* of the element ij.

[3] When a node is fixed to earth, the corresponding entry in $\mathbb{p}$ carries a fixed value; in computations we may choose to reduce the size of the matrix Π by omitting rows which correspond to such fixed nodes. Likewise, we may remove any "edge" which consists of two fixed nodes.

[4] Geometricians term by "rigidity" what we call stability, by "first-order rigidity" what we call rigidity. Our usage is closer to standard engineering terminology.

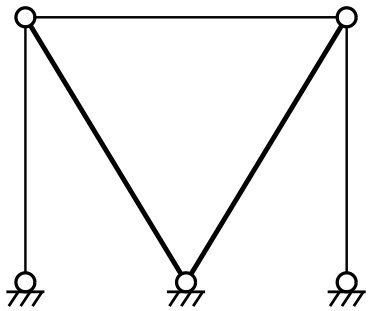

Figure 2. A two-dimensional tensegrity structure.

stress vector $\boldsymbol{\omega}$ that assigns a nonnegative tension to each cable *proper;* if that tension is strictly positive for all cables, we call it *strict.* Second, we must broaden the definition of admissible motion to allow some cables to shorten, although no bar may change length and no cable may lengthen. Correspondingly, the set of admissible velocities for a tensegrity structure will include not only all mechanisms, but also all velocities $\mathbb{v}$ which satisfy

$$\boldsymbol{\pi}_{ij} \cdot \mathbb{v} \leq 0 \tag{9}$$

for all cables, and

$$\boldsymbol{\pi}_{ij} \cdot \mathbb{v} = 0 \tag{10}$$

for all bars.

3.1. ***Expanded kinematics and kinematic criteria for stability.*** To formulate our stability conditions, we must consider motions in more detail. It can be shown that if a motion can occur, one may assume it is real analytic [Glück 1975]. Thus, we can calculate not only its initial velocity $\mathbb{v}$, but also all higher-order derivatives. We follow [Connelly and Whiteley 1996; Alexandrov 2001; Williams 2003] in the calculation of the lengths of edges caused by a motion. Such computations for bar structures date back to Koiter [1984] and Tarnai [1984] , who considered the question of higher-order mechanisms. See also the development in terms of elastic energies in [Salerno 1992] and expansions similar to those below [Vassart et al. 2000].

To formulate the length measure in a convenient way, note that from (4), the edge vector $\boldsymbol{\pi}_{ij}$ (i.e. the column vector of Π) is a linear function of the placement vector $\mathbb{p}$. (11) formalizes this relationship:

$$\boldsymbol{\pi}_{ij}(\mathbb{p}) = B_{ij}\mathbb{p}. \tag{11}$$

It is easy to see that each operator B_{ij} is symmetric. The quantity

$$\lambda_{ij} = B_{ij}\mathbb{p} \cdot \mathbb{p} = \|\boldsymbol{p}_i - \boldsymbol{p}_j\|^2 \tag{12}$$

is the squared length of the edge ij.

We now expand a motion from $\mathbb{p}$

$$\mathbb{q}(t) = \sum_{n=0}^{\infty} t^n \mathbb{q}_n, \tag{13}$$

with coefficients $\mathbb{q}_n$ and with $\mathbb{q}_0 = \mathbb{p}$. For each edge ij, we calculate

$$\lambda_{ij}(t) = B_{ij}\left(\sum_{r=0}^{\infty} t^r \mathbb{q}_r\right) \cdot \left(\sum_{p=0}^{\infty} t^p \mathbb{q}_p\right) = \sum_{r,p=0}^{\infty} t^{r+p} B_{ij}\mathbb{q}_r \cdot \mathbb{q}_p. \tag{14}$$

Let $n = r + p$, so that $p = n - r \geq 0$ and $r \leq n$. The previous expression becomes

$$\sum_{r,p=0}^{\infty} t^{r+p} B_{ij}\mathbb{q}_r \cdot \mathbb{q}_p = \sum_{n=0}^{\infty}\left(\sum_{r=0}^{n} B_{ij}\mathbb{q}_r \cdot \mathbb{q}_{n-r}\right)t^n. \tag{15}$$

For $n = 0$, the first term of the sum is

$$B_{ij}\mathbb{q}_0 \cdot \mathbb{q}_0 = \lambda_{ij}(\mathbb{p}),$$

and we have

$$\lambda_{ij}(t) = \lambda_{ij}(\mathbb{p}) + \sum_{n=1}^{\infty}\left(\sum_{r=0}^{n} B_{ij}\mathbb{q}_r \cdot \mathbb{q}_{n-r}\right)t^n. \tag{16}$$

First, consider a bar. To be admissible, a motion must satisfy $\dot{\lambda}_{ij} = 0$, or

$$\sum_{r=0}^{n} B_{ij}\mathbb{q}_r \cdot \mathbb{q}_{n-r} = 0, \qquad n = 1, 2, \ldots. \tag{17}$$

Since $B_{ij}\mathbb{q}_0 = \boldsymbol{\pi}_{ij}$ and B_{ij} is symmetric, we have the recurrence

$$2\boldsymbol{\pi}_{ij} \cdot \mathbb{q}_n = -\sum_{r=1}^{n-1} B_{ij}\mathbb{q}_r \cdot \mathbb{q}_{n-r}, \qquad n = 1, 2, \ldots. \tag{18}$$

The first few terms of the recurrence are

$$\begin{aligned} 2\boldsymbol{\pi}_{ij} \cdot \mathbb{q}_1 &= 0, \\ 2\boldsymbol{\pi}_{ij} \cdot \mathbb{q}_2 &= -B_{ij}\,\mathbb{q}_1 \cdot \mathbb{q}_1, \\ 2\boldsymbol{\pi}_{ij} \cdot \mathbb{q}_3 &= -2\,B_{ij}\mathbb{q}_2 \cdot \mathbb{q}_1, \\ 2\boldsymbol{\pi}_{ij} \cdot \mathbb{q}_4 &= -2\,B_{ij}\mathbb{q}_1 \cdot \mathbb{q}_3 - B_{ij}\mathbb{q}_2 \cdot \mathbb{q}_2. \end{aligned} \tag{19}$$

Recall that we abbreviate $\boldsymbol{\pi}_{ij}(\mathbb{p})$ as $\boldsymbol{\pi}_{ij}$. The conditions could also be written in the shorter form

$$\begin{aligned} 2\boldsymbol{\pi}_{ij} \cdot \mathbb{q}_1 &= 0, \\ 2\boldsymbol{\pi}_{ij} \cdot \mathbb{q}_2 &= -\boldsymbol{\pi}_{ij}(\mathbb{q}_1) \cdot \mathbb{q}_1, \\ &\text{etc.} \end{aligned} \tag{20}$$

Furthermore, if all edges are unchanged in length, we can write them as

$$\begin{aligned} 2\Pi^T \mathbb{q}_1 &= 0, \\ 2\Pi^T \mathbb{q}_2 &= -\Pi(\mathbb{q}_1)^T \cdot \mathbb{q}_1, \\ &\text{etc.} \end{aligned} \tag{21}$$

This formalism will be useful below.

For a cable the recurrence is similar, but may terminate after a finite number of terms. The conditions are

$$\sum_{r=0}^{n} B_{ij}\mathbb{q}_r \cdot \mathbb{q}_{n-r} \le 0, \qquad n = 1, 2, \ldots, \tag{22}$$

which yields the recurrence

$$2\boldsymbol{\pi}_{ij} \cdot \mathbb{q}_n \le -\sum_{r=1}^{n-1} B_{ij}\mathbb{q}_r \cdot \mathbb{q}_{n-r}, \qquad n = 1, 2, \ldots, \tag{23}$$

with the understanding that the recurrence terminates at the first n for which the inequality is satisfied.

Thus, the algorithm for a cable is

(1) If $2\boldsymbol{\pi}_{ij} \cdot \mathbb{q}_1 < 0$ holds, then the motion is admissible for that component with no further testing needed.

(2) If $2\boldsymbol{\pi}_{ij} \cdot \mathbb{q}_1 = 0$ but $2\boldsymbol{\pi}_{ij} \cdot \mathbb{q}_2 < -B_{ij}\mathbb{q}_1 \cdot \mathbb{q}_1$, then the motion is admissible for that component with no further testing needed.

(3) If $2\boldsymbol{\pi}_{ij} \cdot \mathbb{q}_1 = 0$ and $2\boldsymbol{\pi}_{ij} \cdot \mathbb{q}_2 = -B_{ij}\,\mathbb{q}_1 \cdot \mathbb{q}_1$ but $2\,\boldsymbol{\pi}_{ij} \cdot \mathbb{q}_3 < -2\,B_{ij}\,\mathbb{q}_2 \cdot \mathbb{q}_1$, then the motion is admissible for that component with no further testing needed, etc.

The simplest way to ensure stability is to rule out expansions of the sort outlined above. Note that the $n = 1$ case from each of (17) and (23) combine to require that $\mathbb{q}_1$ is an admissible velocity. Moreover, if all coefficients in the expansion (13) are zero up to the p-th term, then $\mathbb{q}_p$ satisfies the condition to be an admissible velocity. We denote this coefficient as $\mathbb{v} = \mathbb{q}_p$; then it is appropriate to set $\mathbb{a} = \mathbb{q}_{2p}$, $\mathbb{j} = \mathbb{q}_{3p}$. This gives us Criterion 1:

Criterion 1 (Kinematic Test 1). If there is no nonzero admissible velocity $\mathbb{v}$ for a placement, then the structure is stable in that placement.

The second-order test of Connelly and Whiteley occurs at the next step. If the first nonzero coefficient in the expansion is $\mathbb{v}$ and $\boldsymbol{\pi}_{ij} \cdot \mathbb{v} = 0$, then the next term $\mathbb{a}$ must satisfy

$$2\boldsymbol{\pi}_{ij} \cdot \mathbb{a} \le -B_{ij}\mathbb{v} \cdot \mathbb{v}. \tag{24}$$

Equality is required if the edge is a bar. For a cable, if $\boldsymbol{\pi}_{ij} \cdot \mathbb{v} < 0$, then there is no second-order requirement. Formally, this gives us Criterion 2:

Criterion 2 (Kinematic Test 2). Given a placement, suppose for any admissible velocity $\mathbb{v}$ there is no admissible acceleration, i.e., no $\mathbb{a}$ such that

$$2\boldsymbol{\pi}_{ij} \cdot \mathbb{a} = -B_{ij}\mathbb{v} \cdot \mathbb{v} \quad \text{for each bar} \tag{25}$$

and, for each cable for which $\boldsymbol{\pi}_{ij} \cdot \mathbb{v} = 0$,

$$2\boldsymbol{\pi}_{ij} \cdot \mathbb{a} \le -B_{ij}\mathbb{v} \cdot \mathbb{v}. \tag{26}$$

Then the structure is stable in that placement.

The next test is similar. If the first two nonzero coefficients are admissible, then we look at the next. This gives us Criterion 3:

Criterion 3 (Kinematic Test 3). Given a placement, suppose for any admissible velocity $\mathbb{v}$ and acceleration $\mathbb{a}$, there is no $\mathbb{j}$ such that

$$2\boldsymbol{\pi}_{ij} \cdot \mathbb{j} = -2B_{ij}\mathbb{a} \cdot \mathbb{v} \tag{27}$$

for each bar, and

$$2\boldsymbol{\pi}_{ij} \cdot \mathbb{j} \le -2B_{ij}\mathbb{a} \cdot \mathbb{v} \tag{28}$$

for each cable for which $\boldsymbol{\pi}_{ij} \cdot \mathbb{v} = 0$ and $2\boldsymbol{\pi}_{ij} \cdot \mathbb{a} = -B_{ij}\mathbb{v} \cdot \mathbb{v}$. Then the structure is stable in that placement.

The extension to higher orders is straightforward.

Alexandrov's more elaborate conditions [2001] for bar structures can also be extended to tensegrity structures.

3.2. ***Stress tests.*** The direct tests of the last section are not easy to implement; here we discuss simpler tests.

First, consider the simplest form of a stress test. Given a placement $\mathbb{p}$, suppose that there is a mechanism $\mathbb{v}$, and we want to see whether there is a continued second-order term which conserves edge lengths. Equations (25) and (26) seek a solution $\mathbb{a}$ to

$$2\Pi(\mathbb{p})^T\mathbb{a} = -\Pi(\mathbb{v})^T\mathbb{v}. \tag{29}$$

By a standard argument in linear algebra, there is a solution if and only if the right-hand side is perpendicular to all solutions of the homogeneous equation $\Pi(\mathbb{p})\boldsymbol{\omega} = \mathbf{0}$. Thus (29) has a solution if and only if, for all self stresses,

$$\boldsymbol{\omega} \cdot \Pi(\mathbb{v})^T\mathbb{v} = \Pi(\mathbb{v})\boldsymbol{\omega} \cdot \mathbb{v} = 0. \tag{30}$$

If for some self stress this does not hold, the expansion of the motion cannot be continued beyond the first order.

The generalization of this result to tensegrity structures depends on the following extension of the orthogonality test, which relates convex sets rather than subspaces:

Proposition 1. Given a placement and some $\boldsymbol{\epsilon} \in \mathbb{R}^k$, there exists a velocity $\mathbb{w}$ such that, for every bar,

$$\boldsymbol{\pi}_{ij} \cdot \mathbb{w} = \epsilon_{ij}, \tag{31}$$

and for every cable,

$$\boldsymbol{\pi}_{ij} \cdot \mathbb{w} \le \epsilon_{ij}, \tag{32}$$

if and only if, for every proper self stress $\boldsymbol{\omega}$,

$$\boldsymbol{\omega} \cdot \boldsymbol{\epsilon} \ge 0. \tag{33}$$

A proof of this can be found in [Williams 2003; Connelly and Whiteley 1996].

A useful corollary of this is the *zero-self stress condition* due to Roth and Whiteley [1981]: there is an admissible velocity which shortens a particular cable if and only if all self stresses leave that cable unstressed.

From (33), replacing ϵ_{ij} by $-B_{ij}\,\mathbb{v}\cdot\mathbb{v}$, we deduce a criterion for continuing an expansion past the first term $\mathbb{v}$. Namely, for all self stresses $\boldsymbol{\omega}$,

$$\boldsymbol{\omega}\cdot\,\Pi(\mathbb{v})^T\mathbb{v} = \Pi(\mathbb{v})\boldsymbol{\omega}\cdot\,\mathbb{v} \le 0. \tag{34}$$

This leads to:

Criterion 4 (Second-order stress test). Given a placement, if for each admissible velocity $\mathbb{v}$ there is a self stress $\boldsymbol{\omega}$ such that

$$\Pi(\mathbb{v})\boldsymbol{\omega}\cdot\,\mathbb{v} > 0, \tag{35}$$

then the structure is stable in that placement.

A cleaner form of the above computation is given if we define the so-called *stress operator*. This operator is the basis of the force density method. For a given stress vector $\boldsymbol{\omega}$, the self-equilibrium equation (6) becomes

$$\sum \omega_{ij} B_{ij}\mathbb{p} = \Omega\mathbb{p} = 0,$$

and can be regarded as a condition to be satisfied by the nodal coordinates. Due to the form of the operator B_{ij}, this condition is invariant under affine transformations of the nodal coordinates [Connelly and Whiteley 1996; Williams 2003]. We have

$$\Omega := \sum_{\text{edges}} \omega_{ij} B_{ij}, \tag{36}$$

so that

$$\Pi(\mathbb{v})\boldsymbol{\omega}\cdot\,\mathbb{v} = \Omega\mathbb{v}\cdot\,\mathbb{v}. \tag{37}$$

A simple computation then gives the following useful form for (35):

$$\Omega\mathbb{v}\cdot\,\mathbb{v} = \sum_{\text{edges}} \omega_{ij}(\mathbb{v}_i - \mathbb{v}_j)^2 > 0. \tag{38}$$

Calladine and Pellegrino [1991] give a physical motivation for this criterion. If the admissible velocity $\mathbb{v}$ is regarded as an infinitesimal perturbation of $\mathbb{p}$, the perturbed geometric matrix is

$$\Pi(\mathbb{p}+\mathbb{v}) = \big[\ldots \boldsymbol{\pi}_{ij}(\mathbb{p}) + \boldsymbol{\pi}_{ij}(\mathbb{v})\ldots\big] = \Pi(\mathbb{p}) + \Pi(\mathbb{v}). \tag{39}$$

Here, $\boldsymbol{\omega}$ is a prestress for $\mathbb{p}$ but not necessarily one for the placement $\mathbb{p}+\mathbb{v}$. The force which would be required to maintain $\boldsymbol{\omega}$ in the new placement, that is, the so-called *geometric load vector*, would be

$$\mathbb{f} = \Pi(\mathbb{p}+\mathbb{v})\boldsymbol{\omega} = \Pi(\mathbb{v})\boldsymbol{\omega} = \sum \omega_{ij} B_{ij}\mathbb{v}. \tag{40}$$

Given that, (35) can be interpreted as

$$\mathbb{f}\cdot\,\mathbb{v} > 0. \tag{41}$$

This states that positive work must be done to move the structure from its original placement. In other words, the structure possesses first-order positive stiffness.

If the second-order stress test is not satisfied, we can pass to higher-order tests. The next few are (see [Williams 2003])

$$\begin{aligned} \sum \omega_{ij} B_{ij} \mathbb{q}_1 \cdot \mathbb{q}_2 &> 0, \\ 2\sum \omega_{ij} B_{ij} \mathbb{q}_1 \cdot \mathbb{q}_3 + \sum \omega_{ij} B_{ij} \mathbb{q}_2 \cdot \mathbb{q}_2 &> 0, \\ \sum \omega_{ij} B_{ij} \mathbb{q}_1 \cdot \mathbb{q}_4 + \sum \omega_{ij} B_{ij} \mathbb{q}_2 \cdot \mathbb{q}_3 &> 0. \end{aligned} \tag{42}$$

A final result, due to Roth and Whiteley [1981], is proved by different methods (see [Williams 2003], for instance). It says that when $\Pi(\mathbb{p})$ satisfies the condition of maximal independence of column vectors, that is, when the evaluation at $\mathbb{p}$ produces a local maximum for the span of each subset of its column vectors (in their terms, when $\mathbb{p}$ is a *general placement*), the placement is stable if and only if it admits no admissible velocity. The argument is that under these conditions an admissible velocity always can be extended to a motion. We may refer to this as the **maximal-independence test**. Note, in particular, that the criterion is satisfied when the set of all column vectors is linearly independent.

3.3. ***Example.*** An instructive example is shown in Figure 3. In placement (a), if all edges are bars, the

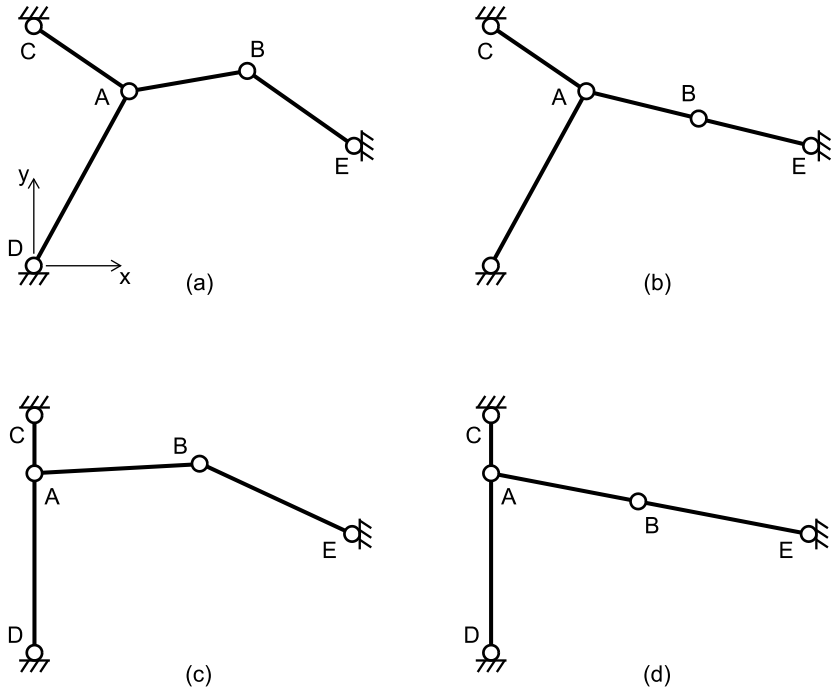

Figure 3. A four-edge example.

placement is stable and unstressed. To verify this, note that the geometric matrix is square:

$$\Pi(\mathbb{q}) = \begin{matrix} \\ A \\ B \end{matrix} \begin{matrix} \begin{matrix} AC & AD & AB & BE \end{matrix} \\ \begin{bmatrix} \boldsymbol{q}_A - \boldsymbol{q}_C & \boldsymbol{q}_A - \boldsymbol{q}_D & \boldsymbol{q}_A - \boldsymbol{q}_B & \mathbf{0} \\ \mathbf{0} & \mathbf{0} & \boldsymbol{q}_B - \boldsymbol{q}_A & \boldsymbol{q}_B - \boldsymbol{q}_E \end{bmatrix} \end{matrix} \tag{43}$$

and, with the placement as illustrated, it is clear that the column vectors must be linearly independent, so the matrix is of full rank and admits neither self stress nor mechanism.

But, in the position shown, or any other in which no edges are collinear, if any of the edges is a cable, the structure is unstable. Physically, this is obvious; analytically, we note that since the placement admits no self stress, by the zero-self stress condition there is an admissible velocity which shortens the cable, and since the edge vectors are linearly independent, the maximal-independence test ensures that the structure is unstable.

If we adjust vertex B as in (b), rendering the edges AB and BE collinear, then the rank of the geometric matrix drops to three, so that both a self stress and a mechanism exist. The mechanism assigns velocity zero to node A, and a nonzero velocity, normal to the $AB - BE$ line, to node B. It is easy to see that all components of the self stress are of the same sign; we may choose them positive in order to use (35) to deduce stability. Any or all of the elements may be converted to cables and stability still is ensured.

Repositioning A as in placement (c), making AC and AD *vertical* and hence collinear, a different situation obtains, with only AC and AD stressable, regardless of the position of B. In this case there is a mechanism, moving both free nodes, but the stability analysis above still holds with AC and AD that can be converted to cables.

A final variation is placement (d), with AC and AD vertical and AB and BE collinear. In this placement, again we can stress only AC and AD. If AB and BE are bars, then the only *mechanism* affects only B, with motion of A occurring at the second order (zero velocity, nonzero acceleration). The interesting computation is that (38) now reveals the second-order stress test to fail. If we calculate the acceleration $\mathbb{a}$ as in (24) (with equality), it is easy to use the next test (42) to discover the stability of this placement. On the other hand, if either AB or BE is a cable, then there is another *admissible velocity*, which is not a mechanism: A can begin to move horizontally while the cable shortens. Again, one can calculate that the placement is stable in this case.

As noted earlier, the second-order test is not a necessary condition for stability, as shown for placement (d), while it is necessary and sufficient for placements possessing first-order positive stiffness, like those in (b) and (c).

4. Sets of stable placements and the rank-deficiency manifold

We have seen that simple rules based only on the topology of a structure cannot generate a generic placement that ensures the stability of a tensegrity structure. This suggests that geometric information is also needed in order to solve the form-finding problem. In this section we consider the structure of some collections of placements, emphasizing the differences between bar structures and tensegrity structures. The characterizations are incomplete, but can serve for prescribing evolution of structures between stable placements. In particular, we focus on the rank-deficient manifold of classical tensegrity structures and

describe differential equations which hold for paths on the manifold. Section 5 then describes a numerical algorithm for solving these equations.

4.1. ***Case 1:*** $\mathbf{\Pi}(\mathbb{p})$ ***has maximal rank.*** First, consider placements in which the $k \times 3n$ geometric matrix is over-square (i.e., $k > 2n$ for two-dimensional structures, and $k > 3n$ for three-dimensional structures) and the rank is maximal. There are self stresses, but there can be no mechanisms. In this case the structure always is stable if it is a bar structure, but if it includes cables it may be unstable. For example, consider the solid-line structure in Figure 3 (a) with an edge AE added, and suppose one of AB or BE a cable. However, if the placement admits a strict proper self stress then the structure is guaranteed to be rigid and hence is stable.

The set of maximal-rank placements is open, since it is the nonzero set of a determinant. Within this set, the set with strict proper self stresses is open.

Next, suppose that $k \leq 3n$ (in the three-dimensional case, or $k \leq 2n$ in the two-dimensional case), and the matrix is of rank k. For a bar structure, there are two cases. If $k = 3n$, then there is no mechanism, and hence the structure is stable. If $k < 3n$ there is a mechanism and because the matrix is maximum rank this means the placement is unstable. For a tensegrity structure, in either case, the absence of a self stress ensures that there is an admissible velocity. Since the rank is maximum it follows that the placement is unstable.

4.2. ***Case 2:*** $\mathbf{\Pi}(\mathbb{p})$ ***has less than maximal rank. The rank-deficiency manifold.*** This is the more subtle and interesting case. Recall that m denotes the number of mechanisms and s the number of self stresses, so that

$$k - s = 3n - m. \tag{44}$$

For a given structure, consider placements in which the rank of Π is r. It is easy to see that the collection of all these placements form a smooth manifold in $\mathbb{R}^{3n}$. (As we verify below, it can happen that the manifold intersects itself.) However, it is a little more difficult to show that at each point on the manifold, the tangent plane consists of the vectors normal to

$$\mathbb{n} := \sum \omega_{ij} B_{ij} \mathbb{v} = \Pi(\mathbb{v})\boldsymbol{\omega} = \Omega \mathbb{v}, \tag{45}$$

for all choices of self stress $\boldsymbol{\omega}$ and mechanisms $\mathbb{v}$ at the point (see [Williams 2003]). The set of all the normal vectors[5] (45) span a subspace which we will denote as $\mathbb{N}$.

We consider a placement on the manifold at which the second-order stress test holds. There are three subspaces of interest of $\mathbb{R}^{3n}$:

- $\mathbb{V} = \text{Nullspace}(\Pi(\mathbb{p})^T)$, the subspace of mechanisms;
- $\mathbb{N} = \Omega(\mathbb{p})\mathbb{V}$, the subspace of normal vectors;
- $\mathbb{P} := \text{Range}(\Pi(\mathbb{p})) = \text{span}\{\boldsymbol{\pi}_{ij}(\mathbb{p})\}$.

Since the second-order test ensures that $\Omega \mathbb{v} \cdot \mathbb{v} \neq 0$ for all $\mathbb{v} \in \mathbb{V}$, it follows that the nullspace of Ω does not intersect $\mathbb{V}$. Thus,

$$\dim(\mathbb{N}) = \dim(\mathbb{V}) = 3n - \dim(\mathbb{P}). \tag{46}$$

[5]Notice that this is the geometric load vector of (40).

However, the test also implies that $\mathbb{N}$ and $\mathbb{P}$ share only the zero vector. Otherwise, if $\mathbb{n} = \Omega\mathbb{v}$ were in both, we would need $\mathbb{v} \cdot \Omega\mathbb{v} = 0$. Hence $\mathbb{N}$ and $\mathbb{P}$ are complementary subspaces, although in general not orthogonal. It follows that the orthogonal projection of $\mathbb{P}$ onto the tangent space of the manifold along $\mathbb{N}$ is the entire tangent space.

Next, note that (11) and (12) imply that $2\boldsymbol{\pi}_{ij}$ is the gradient vector of $\boldsymbol{\lambda}_{ij}$. Our argument shows that when these edge vectors are projected onto the tangent space, they span that space. By assumption, they are linearly dependent; we may extract a linearly independent subset which will form a basis for the tangent space. This means that the corresponding edge lengths form a local coordinate system on the manifold. We will use this observation to prescribe paths traversing the manifold.

4.3. ***An example of self-intersection.*** Consider the structure in Figure 3. For a simple computation we set

$$\mathbb{p}_D = (0, 0), \quad \mathbb{p}_C = (0, 2), \quad \mathbb{p}_E = (3, 1), \quad \mathbb{p}_A = (x_A, y_A), \quad \mathbb{p}_B = (x_B, y_B). \tag{47}$$

The matrix Π is square, so that the rank-deficient placements are found from $\det \Pi = 0$. The latter may be written explicitly as

$$x_A\,(x_B + x_A y_B - x_A - x_B y_A - 3y_B + 3y_A) = 0. \tag{48}$$

Thus $x_A = 0$ describes one manifold segment, which may be parameterized by y_A, x_B, y_B. Another manifold segment is

$$y_B = (x_B y_A - x_B + x_A - 3y_A)/(x_A - 3), \tag{49}$$

which can be parameterized by x_A, y_A, x_B. These two three-dimensional manifolds (in $\mathbb{R}^4$) meet in a two-dimensional manifold and clearly are not parallel at the intersection. The placement at this intersection is that shown in Figure 3 (d); it can be parameterized by y_A and x_B.

At points on the two-dimensional intersection manifold, the normal vector calculation (45) yields only null vectors, but nonetheless it is possible to traverse through the point on one of the branches of the manifold since the normals continue smoothly on either side of the intersection.

4.4. ***Paths traversing the manifold.*** The only case which is simple to treat is that of one mode of self stress (that is, s=1), so we consider only that case. We continue to assume that we have a placement $\mathbb{p}$ at which the second-order stress test is satisfied. Starting from this placement on the manifold, by the continuity of the nullspaces, there is a neighborhood on the manifold where the second-order test is satisfied and $s = 1$. Hence, the placements are stable. We consider how to construct paths on the manifold which stay within this neighborhood.

The first condition will ensure that the path $\mathbb{q}(t)$ is on the manifold. We require that, for each normal vector $\mathbb{n}$ at the placement $\mathbb{q}(t)$,

$$\dot{\mathbb{q}} \cdot \mathbb{n} = 0. \tag{50}$$

Recall that $\dot{\mathbb{q}}$ denotes the nodal velocities when we are moving from one placement to another, and $\mathbb{v}$ denotes a mechanism in a given placement. The rate of change in each edge length as we move is

$$\boldsymbol{\pi}_{ij}(\mathbb{q}(t)) \cdot \dot{\mathbb{q}} = \epsilon_{ij}. \tag{51}$$

Since a selection of the edge lengths serves as a coordinate system, we may vary those at will by choosing the appropriate ϵ_{ij} in (51). Then, adding condition (50) we obtain a system of $3n = \dim(\mathbb{P}) +$

dim(ℕ) differential equations for $\mathfrak{q}(t)$, whose solution allows us to compute the other edge lengths using (12). In the next section we detail this process.

Using the stress vector at $\mathfrak{q}(t)$, we have

$$\sum \omega_{ij} \boldsymbol{\pi}_{ij}(\mathfrak{q}(t)) = 0. \tag{52}$$

Taking an inner product results in

$$\sum \omega_{ij} \boldsymbol{\pi}_{ij} \cdot \dot{\mathfrak{q}} = 0, \tag{53}$$

which means that the edge lengths obey

$$\sum \omega_{ij} \dot{\lambda}_{ij} = 2 \sum \omega_{ij} \epsilon_{ij} = 0. \tag{54}$$

This condition restricts the relative change of the edge lengths at each point along the path. Recall that $\omega_{ij} = \tau_{ij}/\ell_{ij}$ and $\epsilon_{ij} = \ell_{ij}\, \dot{\ell}_{ij}$, with ℓ_{ij} being the length of the edge ij. Therefore, this condition takes the form $\sum \tau_{ij}\, \dot{\ell}_{ij} = 0$, meaning that the internal forces spend no power on the path.

Since the self stress vector also represents the vector of incompatible lengthenings (see [Pellegrino and Calladine 1986]), that is, those which do not preserve the connectivity of the structure, (54) can be seen as the orthogonality condition between $\boldsymbol{\epsilon}$ and the incompatible lengthenings. It is identically satisfied if (50) holds.

5. The marching procedure

In this section, we describe how to create a path along the rank-deficiency manifold. As before, we restrict ourselves to the case $k \leq 3n$ and $s = 1$, and assume that we are proceeding from a placement which satisfies the second-order stress test. The path on the manifold $\mathfrak{q}(t)$ is determined as the solution of the system of differential equations (50) and (51).

5.1. ***The system of equations.*** Since the dimension of the subspace of self stresses is one, we write $\dim(\mathbb{P}) = k - 1$ equations, assigning to each of $k - 1$ edge vectors the derivative of its length. By the complementarity of ℕ and ℙ, we can complete the differential system with the normal conditions between $\dot{\mathfrak{q}}$ and the $3n - k + 1 = \dim(\mathbb{N})$ independent normal vectors.

The simplest marching process involves changing the length of only two edges, say ab and cd. To move away from the starting placement, we change the length of ab at a designated rate ϵ_{ab}. For a generic edge $hk \neq ab, cd$, the length derivative is set equal to zero. For this process, we solve for $\mathfrak{q}(t)$ the system

$$\left\{ \begin{array}{ll} \boldsymbol{\pi}_{ab} \cdot \dot{\mathfrak{q}} = \epsilon_{ab} & \\ \boldsymbol{\pi}_{hk} \cdot \dot{\mathfrak{q}} = 0 & \forall\, hk \neq ab, cd \\ \mathfrak{n} \cdot \dot{\mathfrak{q}} = 0 & \forall\, \mathfrak{n} \in \mathbb{N} \end{array} \right\}, \tag{55}$$

and then calculate the change in length of the other chosen edge, cd.

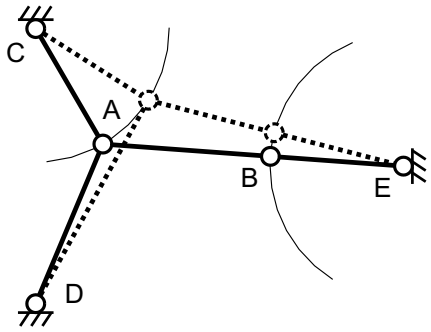

Figure 4. Moving from one placement to another.

As an example, consider the solid-line placement in Figure 4 for which we change the lengths of AB and CD, with $\epsilon_{AB} < 0$. The change of length of AD is determined by the solution to the system

$$\left\{\begin{array}{l} \boldsymbol{\pi}_{AB} \cdot \dot{\mathfrak{q}} = \epsilon_{AB} \\ \boldsymbol{\pi}_{AC} \cdot \dot{\mathfrak{q}} = 0 \\ \boldsymbol{\pi}_{BE} \cdot \dot{\mathfrak{q}} = 0 \\ \mathfrak{n} \cdot \dot{\mathfrak{q}} = 0 \end{array}\right\}. \tag{56}$$

With these settings the nodes A and B follow the thin solid-line circular trajectories; the normal condition ensures that AB and BE remain collinear and AD is lengthened accordingly, as shown by the dotted-line placement.

Often it is desirable to change the lengths of many edges at the same time, for example in order to preserve some symmetry. In such a case, we might choose two disjoint subsets $\mathscr{E}_1$, $\mathscr{E}_2$, of k_1, k_2 edges respectively, and assign the same changes in length, ϵ_1 and ϵ_2 respectively, to each edge in each group. In this case we have the system

$$\left\{\begin{array}{ll} \boldsymbol{\pi}_{ij} \cdot \dot{\mathfrak{q}} = \epsilon_1 & \forall\, ij \in \mathscr{E}_1 \\ \boldsymbol{\pi}_{hk} \cdot \dot{\mathfrak{q}} = 0 & \forall\, hk \in \mathscr{E} \setminus \{\mathscr{E}_1 \cup \mathscr{E}_2\} \\ (\boldsymbol{\pi}_{fg} - \boldsymbol{\pi}_{lm}) \cdot \dot{\mathfrak{q}} = 0 & \forall\, fg, lm \in \mathscr{E}_2 \\ \mathfrak{n} \cdot \dot{\mathfrak{q}} = 0 & \forall\, \mathfrak{n} \in \mathbb{N} \end{array}\right\}. \tag{57}$$

The unknown change in length ϵ_2 is then obtained from the solution of this system.

Analogously, for general cases, we can choose different length derivatives, within each subset $\mathscr{E}_1$ and $\mathscr{E}_2$, setting those in $\mathscr{E}_1$ directly, and those in $\mathscr{E}_2$ to be proportional to an assigned vector $\boldsymbol{\epsilon}_2 = \alpha\bar{\boldsymbol{\epsilon}}$. Thus we write for these edges the $k_2 - 1$ independent equations of the form

$$(\boldsymbol{\pi}_{fg} - \frac{\bar{\epsilon}_{fg}}{\bar{\epsilon}_{lm}}\boldsymbol{\pi}_{lm}) \cdot \dot{\mathfrak{q}} = 0. \tag{58}$$

As before, the unknown parameter α is obtained from the solution of the differential system.

5.2. ***Limiting placements.*** Next, we consider possible difficulties which arise when one deals with the differential system (55), choosing to vary only two lengths. In the previous example in Figure 4 it

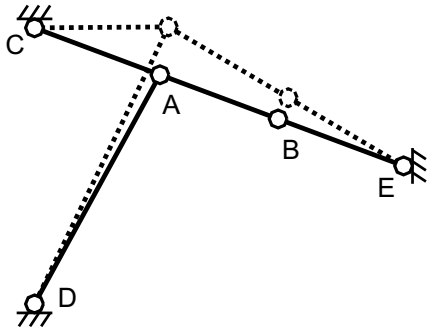

Figure 5. Moving from a limit placement.

is not possible to shorten AB indefinitely, because its length can reach a minimum value. This value corresponds to the *limit placement* represented by the solid-line in Figure 5, where the three edges AC, AB and BE are collinear. It is easy to see that this limit placement occurs at a smooth point of the rank-3 manifold, so this does not represent a break in the manifold.

Moreover, starting from the limit placement and lengthening the edge AB, there exist two possible paths on the manifold, advancing toward either the dotted-line placement in Figure 4 or that in Figure 5.

The important fact is that the edge AD is unstressed in the limiting placement. Calling the subsystem composed of all stressed edges a *minimal subsystem*, we discover that we cannot arbitrarily assign the lengthenings of all edges belonging to such a subsystem. Indeed, from (53) or (54), we have

$$0 = \omega_{AD}\boldsymbol{\pi}_{AD} \cdot \dot{\mathbb{q}} + \omega_{AB}\boldsymbol{\pi}_{AB} \cdot \dot{\mathbb{q}} = \omega_{AD}\epsilon_{AD} + \omega_{AB}\epsilon_{AB}, \tag{59}$$

since the edges AC and BE do not change in length. This relation shows that, since in the limit placement $\omega_{AD} = 0$ and $\omega_{AB} \neq 0$, the lengthening of AB must be zero. This example illustrates the role that stresses play while moving along the rank-deficiency manifold. When the edges that change their lengths have stresses of the same sign, one edge shortens and the other lengthens (see Figure 4); when the stresses are of opposite sign, they both lengthen or shorten (see Figure 5).

As a second example, consider the structure in Figure 6. We assign a positive lengthening to AD and zero lengthening to AB and BE, while the lengthening of AC is to be determined. The normal condition requires that AC and AD remain aligned. Following these rules we arrive at the dotted-line limit placement: AD cannot be further lengthened since AB and BE are aligned. In this case, both ω_{AB} and ω_{BE} are zero throughout the process.

This is a different type of limit placement in that, as noted earlier, it belongs to the intersection of two rank-deficiency manifolds. The tangent space is undefined on this intersection and the computation of the normal vector gives a null vector as a result. Progress from this placement requires a commitment to one branch or the other of the manifold, and the corresponding normals must be selected as the limit of those from adjacent placements.

5.3. ***Implementation in MATLAB.*** The MATLAB programming package has been employed for numerical computations, for both the stability analysis and the marching process.

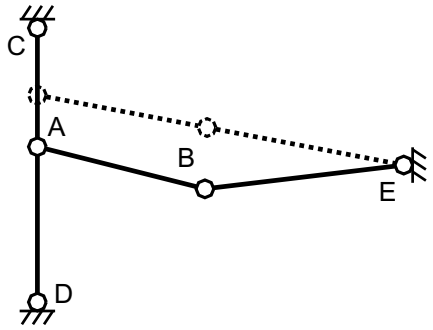

Figure 6. Another limit placement.

Figure 7 shows the flowchart that summarizes our analysis on a given system. Here is the sequence of steps:

- In Step 1, the collection of nodes and edges is assigned, and some of the nodes are constrained to fixed locations. Here n represents the number of free nodes. The vector $\mathbb{p}$ contains all (free and fixed) nodal coordinates, so that any vector representing velocities or higher order derivatives contains zeros as fixed entries.
- In Step 2, we construct the matrix $\Pi(\cdot)$ as a function that can be evaluated at any nodal placement.
- In Step 3, the rank of the geometric matrix $\Pi(\mathbb{p})$ is computed; this gives also the dimensions s and m of the nullspaces of self stresses and mechanisms.
- With this information we can pass through tests from step 4 to step 7 to identify the system type. For a full-rank geometric matrix (tests 4–6), we have three cases:
  - For a square matrix, the system is stable if and only if there are no cables;
  - For $s > 0$, the system is stable if and only if there is a positive self stress in all cables;
  - For $m > 0$ the system is unstable.

  The last test checks for a submaximal rank with $s = 1$; this is to exclude more complicated situations, whose methodology of analysis will be outlined in a later paper.
- In Step 8, we compute the quantity $\Omega\, \mathbb{v} \cdot \mathbb{v}$ from the self stress and the mechanisms of the system.
- In Step 9, we perform the second-order test to be ready for the marching process. To this end, it is sufficient to test the positivity of a reduced matrix $\hat{\Omega}$ whose (h, k) entry is the scalar product of the h-th independent normal vector with the k-th independent mechanism.
- If the test fails, then we perform Step 10: If $\hat{\Omega}$ is positive semidefinite we need a higher-order analysis. Otherwise the system is definitely unstable.
- We now can choose the two subsets of edges $\mathscr{E}_1$ and $\mathscr{E}_2$ in Step 11 and assign their lengthenings (Step 12).
- In step 13, we check that the chosen set of prescribed lengthenings $\mathscr{E}\backslash\mathscr{E}_2$ is not a minimal subsystem, otherwise we need to modify our choice in step 11.

- Finally, in step 14, we solve the system of differential equations. Recall that the stability of the placements on the resulting path is ensured only in a neighborhood of the starting placement, hence, it is ensured only for sufficiently small changes of the length of the elements.

The MATLAB built-in function `ode45` can be used to solve the differential system numerically. This function employs the Runge–Kutta method and solves systems of the form

$$\mathbf{M}(\mathbb{q}, t)\dot{\mathbb{q}} = \mathbf{f}(\mathbb{q}, t),$$

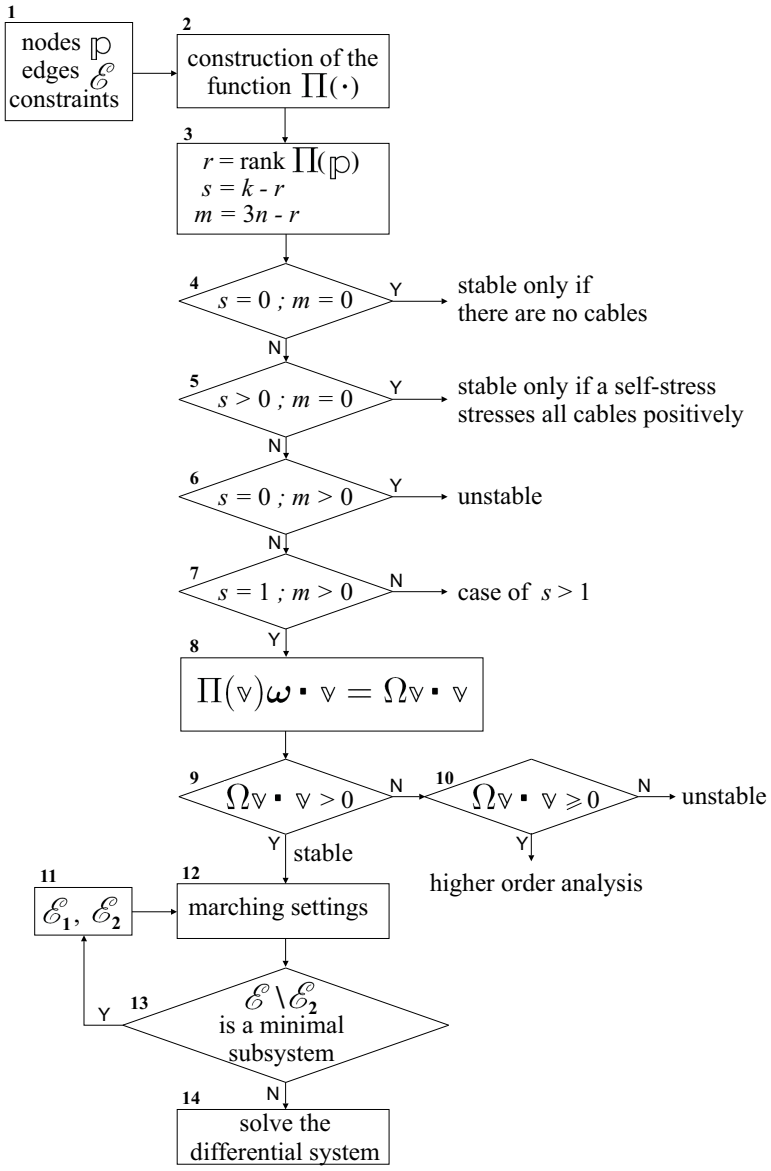

Figure 7. Flowchart for the algorithm.

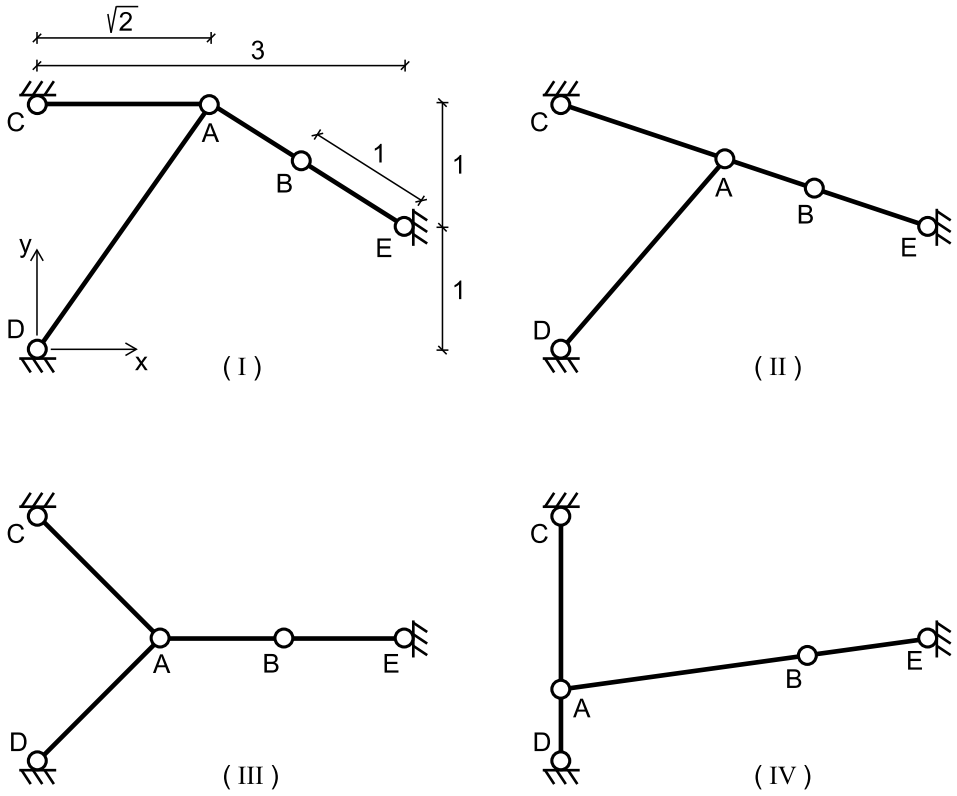

Figure 8. Sample calculations.

in which **M** is the so-called mass matrix and **f** is the vector of known terms. According to (57) and (58), here the rows of **M** are the edge vectors, the linear combinations of them and the normal vectors; the entries of **f** are the corresponding lengthenings and zeros.

In step 3 and during step 14, the rank of the geometric matrix and the associated nullspaces are computed using the singular value decomposition, through the MATLAB function `svd` (see [Pellegrino 1993]). This function gives the sets of singular vectors and the (positive) singular values in decreasing order. The singular values that are close to zero correspond to the corank $\min(3n, k) - r$ of the geometric matrix; the singular values then represent a measure of how close the placement is to the rank-deficiency manifold. For analytically determined rank-deficient placements, these values are of the order of 10^{-14} or lower. During the resolution of the differential system ($s = 1$) the unique value close to zero may grow but it is found that the ratio with the previous one remains at least of the order 10^{-3}. Usually this ratio grows excessively when the marching process requires the system to pass through a limit placement.

5.4. ***Numerical computations.*** We present some results for the example of Figure 3. The coordinates of constrained nodes are given as in Section 4.3; edges AC and BE have fixed length equal to $\sqrt{2}$ and 1 respectively.

Initial-final placement	Independent nonnull lengthening	Maximum error on final coordinates $\Delta x_P = x_{P,num} - x_{P,an}$	Singular values ratio
I-II	$\epsilon_{AB} < 0$	$\lvert\Delta y_A\rvert \simeq 3 \cdot 10^{-3}$	10^{-10}
I-II	$\epsilon_{AD} < 0$	$\lvert\Delta x_B\rvert \simeq 4 \cdot 10^{-12}$	10^{-12}
I-III	$\epsilon_{AD} < 0$	$\lvert\Delta y_B\rvert \simeq 3 \cdot 10^{-9}$	10^{-10}
III-I	$\epsilon_{AD} > 0$	$\lvert\Delta x_B\rvert \simeq 10^{-9}$	10^{-9}
II-III	$\epsilon_{AD} < 0$	$\lvert\Delta x_A\rvert \simeq 2 \cdot 10^{-10}$	10^{-11}
III-II	$\epsilon_{AB} < 0$	$\lvert\Delta y_A\rvert \simeq 3 \cdot 10^{-3}$	10^{-9}
III-II	$\epsilon_{AD} > 0$	$\lvert\Delta x_A\rvert \simeq 4 \cdot 10^{-11}$	10^{-11}
I-IV	$\epsilon_{AD} < 0$	$\lvert\Delta x_A\rvert \simeq 2 \cdot 10^{-3}$	10^{-8}
II-IV	$\epsilon_{AD} < 0$	$\lvert\Delta x_A\rvert \simeq 2 \cdot 10^{-3}$	10^{-8}
III-IV	$\epsilon_{AD} < 0$	$\lvert\Delta x_A\rvert \simeq 10^{-3}$	10^{-10}
III-IV	$\epsilon_{AB} > 0$	$\lvert\Delta y_B\rvert \simeq 5 \cdot 10^{-3}$	10^{-7}

Table 1. Numerical results.

Figure 8 shows four different placements; we pass from one to another of these placements by changing the lengths of AD and AB. The last placement lies on the self-intersection of the manifold, while the other three belong to the part of the manifold represented by (49). In particular, in the first position (I) the edge AC is horizontal; the second position (II) correspond to the first kind of limit placement discussed in 5.1; in the third position (III) edges AB and BE are aligned horizontally. Edges AC and BE are fixed in length and their corresponding independent lengthening are zero. The last independent lengthening can be assigned to AD or AB by using the relation

$$\epsilon_{ij}\Delta t = \tfrac{1}{2}(\ell^2_{ij,fin} - \ell^2_{ij,in}), \tag{60}$$

which is obtained by integrating the equation

$$\ell_{ij}\dot{\ell}_{ij} = \text{const} = \epsilon_{ij},$$

and relating the initial and final length of an element with its lengthening during an interval of time. For processes starting from (or passing through) position II, we are forced to assign the lengthening of AD, because we cannot fix all the lengthenings of the minimal subsystem $\{AC, AB, BE\}$. Recall that if we want to start a process from placement IV, we need to provide the initial normal vector.

Table 1 shows some results for different marching processes between the placements; the result are obtained by the MATLAB solver with default settings. For each process we report the maximum difference between analytically and numerically computed final nodal coordinates. We also report the order of the ratio between the last two singular values of the geometric matrix in the final placement; this ratio is of the order of 10^{-17} at the beginning of each process. If the final placement is the limit placement II (processes I-II and III-II), when the independent lengthening is that of AB, then the error on the coordinates may grow up to 10^{-3}: the limiting placement cannot be reached as accurately since the independent length reaches a minimum value. This is also the case of processes that end in the limit

placement IV with independent lengthening of AD. The last case III-IV with independent lengthening of AB gives worse results, this is due to the nonexistence of the normal vector in placement IV.

We end by showing an application of the method to a large three-dimensional structure. We applied the marching procedure to a tensegrity tower, the kind of decorative structure often realized by Snelson. Figure 9 shows an arch-shaped structure obtained from the tower by lengthening (shortening) the cables on the upper (lower) side of the arch. A simplified analytical solution for the form-finding problem of this kind of towers is given in [Micheletti 2003]. It is used to construct the starting placement. For the tower in question, the ratio between the last two singular values is of the order of 10^{-14}. The choice of the edge lengthenings ϵ_{ij} is crucial in order to avoid limiting placements; in some cases we reached the arch-shaped placement but we found this ratio to grow excessively, up to 10^{-2}, and the self stress to take values close to zero in most of the elements. For a careful choice of the process, this ratio can be of the order of 10^{-5} or lower at the final placement; the self stress results then are uniform along the arch and nonzero in each edge.

6. Discussion

We have presented a method for finding one-parameter families of stable placements for tensegrity structures, starting from a known initial stable placement. The method applies to the set of rank-deficient placements which is characterized within a general classification of tensegrity structures. This classification is obtained from an ordered collection of known results which were previously scattered through the mathematical and engineering literature.

After having discussed the case of a full-rank geometric matrix, we have given the characterization of the rank-deficiency manifold through the identification of its normal, (45). We proved that a subset of the edge lengths can be chosen as a local coordinate system on the manifold, Then we have focused on the simple case of a single state of self stress. The kinematic equations (51) relating the nodal velocities $\dot{\mathfrak{q}}$ to the lengthenings ϵ_{ij} of the chosen coordinate system have been used to prescribe a path on the manifold, together with the prescription (50), that the nodal velocities must belong to its tangent space. The resulting differential system was implemented and solved using various MATLAB routines.

The characterization of the manifold is a key feature of the method. It appears to be not known in the literature while some of the existing form-finding methods might benefit of its application. A main advantage, with respect to other approaches, is that the lengths of the elements are directly controlled. This feature makes the method well suited for the rapid analysis of variable geometry structures, such as deployable or tendon controlled systems.

The method can be applied reliably to large structures, in general with multiple mechanisms ($m \geq 1$). The last $(m+1)$ singular values of the geometric matrix serve to measure the accuracy of the placements on the manifold. The accuracy decays as a limit placement is approached.

Condition (54) gives insight into the marching process. It not only establishes the relation between the signs of stresses and lengthenings during a process but also justifies the definition of limit placement and minimal subsystem.

We have shown that the final placement is stable in a neighborhood of a starting stable placement, however in the simulations it is possible to reach stable placements which are very far from the initial

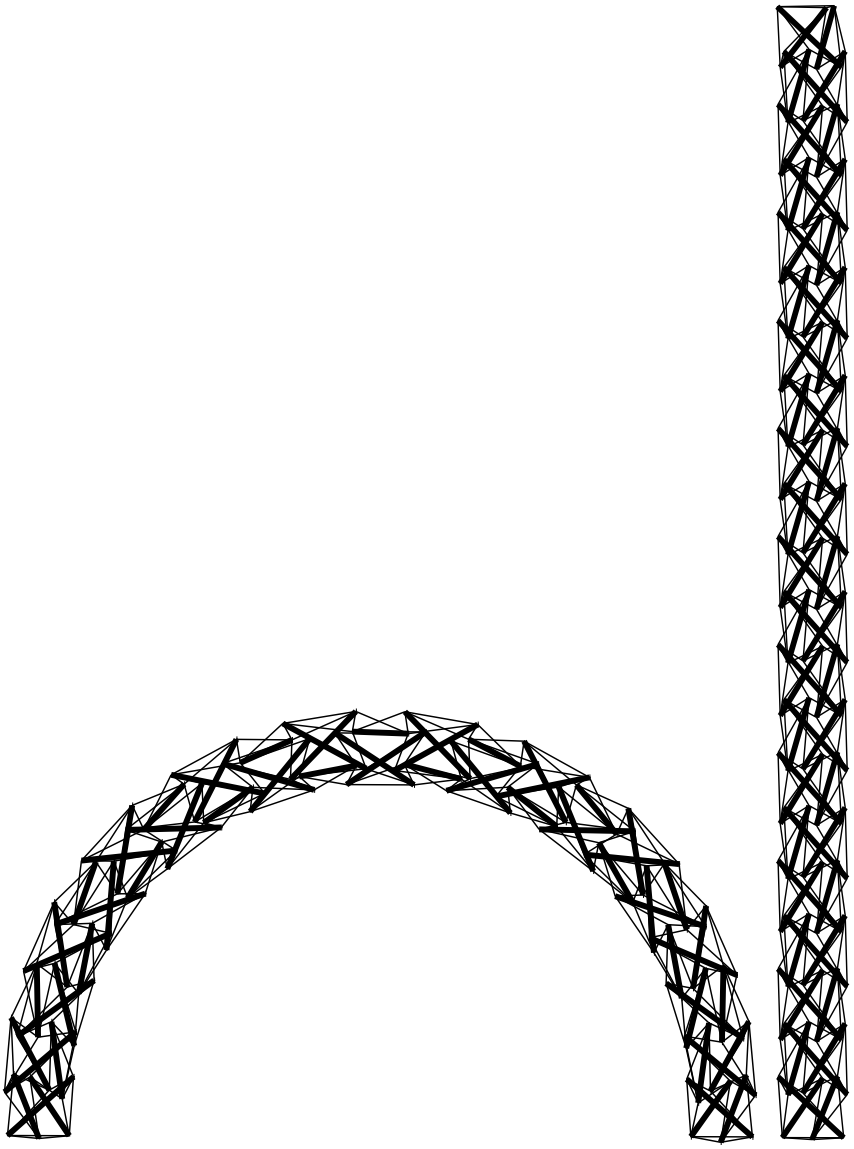

Figure 9. The algorithm was used to transform the tower into this arch.

one. For complicated cases, it can be necessary to test for stability each point of the path to avoid the occurrence of unstable portions.

We remark again that our model considers only rigid bars and inextensible cables connected by pin-joints, so that the material properties of the elements in a corresponding physical structure are not necessary for the form-finding process. On the other hand, local or global buckling instabilities, which depend on the material employed, on the magnitude of the self stress and on magnitude of the external loads, have to be considered separately. However, the stability of a physical realization of a structure satisfying

the second-order stress test can still be ensured by limiting the magnitude of the self stress and/or of the external loads. Regarding the problem of cable-slackening, it is important to avoid placements with an high ratio between the stress in bars and cables.

Concerning future improvements, some aspects are important which are not covered in this paper. A first and straightforward improvement consists in including geometry constraints. They can be easily written in the form $\mathbb{c} \cdot \dot{\mathbb{q}} = 0$, with $\mathbb{c}$ a constant or time dependent vector characterizing the constraint. A second and more difficult task would be the extension of the method to include stress control of some edges. Lastly, a necessary step for forthcoming studies is the development of a procedure in case of multiple states of self stress. In regard to this, we remark that the characterization of the rank-deficiency manifold still holds but the details of such a procedure remain to be outlined.

7. Conclusions

Our procedure offers a simpler approach for discovering the range of feasible geometries for a given topology of a tensegrity structure, given an initial stable placement. It applies to the set of rank-deficient placements. The method is independent of the material properties of the structures. It is especially useful for the development of variable-geometry applications, since it employs the edge lengths as control parameters for movement on a continuous path of stable placements. The characterization of the rank-deficiency manifold provides more insight into the form-finding process then existing approaches. The method can be accurately applied to large structures, and it can be extended to the more complicated case of multiple states of self stress.

Acknowledgements

We thank the reviewers for several useful suggestions.

References

[Aldrich et al. 2003] J. B. Aldrich, R. E. Skelton, and K. Kreutz-Delgado, "Control synthesis for a class of light and agile robotic tensegrity structures", pp. 5245–5251 in *Proceedings of the IEEE American Control Conference, Denver, Colorado*, 2003.

[Alexandrov 2001] V. Alexandrov, "Implicit function theorem for systems of polynomial equations with vanishing jacobian and its application to flexible polyhedra and frameworks", *Monatshafte fur Math* **132** (2001), 269–288.

[Asimow and Roth 1979] L. Asimow and B. Roth, "The rigidity of graphs II", *J. Math. Anal. Appl.* **68** (1979), 171–190.

[Barnes 1999] M. R. Barnes, "Form finding and analysis of tension structures by dynamic relaxation", *Int. J. Space Struct.* **14**:2 (1999), 89–104.

[Bouderbala and Motro 1998] M. Bouderbala and R. Motro, "Folding tensegrity systems", pp. 27–36 in *Proceedings of IUTAM/IASS Symposium on Deployable Structures: Theory and Applications, Cambridge, U.K.*, 1998.

[Burkhardt 2005] R. W. Burkhardt, *A practical guide to tensegrity design*, Second ed., Tensegrity Solutions, Cambridge, Massachusetts, 2005.

[Calladine 1978] C. R. Calladine, "Buckminster Fuller's 'tensegrity' structures and Clerk Maxwell's rules for the construction of stiff frames", *Int. J. Solids Struct.* **14** (1978), 161–172.

[Calladine and Pellegrino 1991] C. R. Calladine and S. Pellegrino, "First-order infinitesimal mechanisms", *Int. J. Solids Struct.* **27** (1991), 505–515.

[Cauchy 1813] A. L. Cauchy, "Sur les polygons et le polyhéders", *XVIe Cahier* **9** (1813), 87–89.

[Connelly and Back 1998] R. Connelly and A. Back, "Mathematics and tensegrity", *American Scientist* **86**:2 (1998), 142–151.

[Connelly and Whiteley 1996] R. Connelly and W. Whiteley, "Second-order rigidity and prestress stability for tensegrity frameworks", *SIAM J. Discrete Math.* **9** (1996), 453–491.

[Day 1965] A. S. Day, "An introduction to dynamic relaxation", *The Engineer* **219** (1965), 218–221.

[Defossez 2003] M. Defossez, "Shape memory effect in tensegrity structures", *Mechanics Research Communications* **30** (2003), 311–316.

[El Smaili et al. 2004] A. El Smaili, R. Motro, and V. Raducanu, "New concept for deployable tensegrity systems, structural mechanics activated by shear force", pp. 318–319 in *Proceedings of IASS04, Int. Association for Shell and Spatial Structures, Montpellier, France*, 2004.

[Estrada et al. 2006] G. G. Estrada, H.-J. Burgardtz, and C. Mohrdieck, "Numerical form-finding of tensegrity structures", *Int. J. Solids Structures* **43** (2006), 6855–6868.

[Fest et al. 2004] E. Fest, K. Shea, and I. F. C. Smith, "Active Tensegrity Structure", *Journal of Structural Engineering* **130**:10 (2004), 1454–1465.

[Furuya 1992] H. Furuya, "Concept of deployable tensegrity structures in space applications", *Int. J. Space Struct.* **7**:2 (1992), 143–151.

[Glück 1975] H. Glück, "Almost all simply connected surfaces are rigid", *Geometric Topology, Lecture Notes in Math, Springer Verlag* **438** (1975), 225–239.

[Hanaor 1993] A. Hanaor, "Double-layer tensegrity grids as deployable structures", *Int. J. Space Struct.* **8**:1–2 (1993), 135–143.

[Koiter 1984] W. T. Koiter, "On Tarnai's conjecture with reference to both statically and kinematically indeterminate structures", Technical Report 788, Laboratory for Engineering Mechanics, Delft, The Netherlands, 1984.

[Linkwitz and Schek 1971] K. Linkwitz and H. J. Schek, "Einige Bemerkungen zur Berechnung von Vorgespanten Seilnetzkonstruktionen", *Ingenieur–Archiv* **40** (1971), 145–158.

[Masic et al. 2006] M. Masic, R. E. Skelton, and P. E. Gill, "Optimization of tensegrity structures", *Int. J. Solids Struct.* **43** (2006), 4687–4703.

[Maxwell 1869] J. C. Maxwell, "On reciprocal diagrams, frames and diagrams of forces", *Trans. Roy. Soc. Edinburgh* **26** (1869), 1–40.

[Micheletti 2003] A. Micheletti, "The indeterminacy condition for tensegrity towers, a kinematic approach", *Rev. Fr. de Génie Civil* **7** (2003), 329–342.

[Möbius 1837] A. F. Möbius, *Lehrbuch der statik vol. 2*, Göschen, 1837.

[Motro 1984] R. Motro, "Forms and forces in tensegrity systems", pp. 180–185 in *Proceedings of 3rd International Conference on Space Structures* (Amsterdam, The Netherlands), 1984.

[Motro 2003] R. Motro, *Tensegrity: structural systems for the future*, Kogan Page Science, London, U.K., 2003.

[Murakami and Nishimura 2001] H. Murakami and Y. Nishimura, "Static and dynamic characterization of regular truncated icosahedral and dodecahedral tensegrity modules", *Int. J. Solids Struct.* **38**:50–51 (2001), 9359–9381.

[Nishimura 2000] Y. Nishimura, *Static and dynamic analyses of tensegrity structures*, Ph.D. thesis, University of California at San Diego, La Jolla, California, 2000.

[Ohsaki and Zhang 2006] M. Ohsaki and J. Y. Zhang, "Stability conditions of prestressed pin-jointed structures", *Int. J. Non-Linear Mechanics* **41** (December 2006), 1109–1117.

[Oppenheim and Williams 1997] I. J. Oppenheim and W. O. Williams, "Tensegrity prisms as adaptive structures", *Adaptive Structures and Material Systems ASME* **54** (1997), 113–120.

[Paul et al. 2005a] C. Paul, H. Lipson, and F. J. V. Cuevas, "Design and control of tensegrity robots for locomotion", *IEEE Transactions on Robotics* **22**:5 (2005), 944–957.

[Paul et al. 2005b] C. Paul, H. Lipson, and F. J. V. Cuevas, "Evolutionary form-finding of tensegrity structures", pp. 3–10 in *Proceedings of the 2005 Genetic and Evolutionary Computation Conference* (Washington, D.C.), 2005.

[Pellegrino 1986] S. Pellegrino, *Mechanics of kinematically indeterminate structures*, Ph.D. thesis, University of Cambridge, U.K., 1986.

[Pellegrino 1992] S. Pellegrino, "A class of tensegrity domes", *Int. J. Space Struct.* **7** (1992), 127–142.

[Pellegrino 1993] S. Pellegrino, "Structural computations with the singular value decomposition of the equilibrium matrix", *Int. J. Solids Struct.* **30** (1993), 3025–3035.

[Pellegrino and Calladine 1986] S. Pellegrino and C. R. Calladine, "Matrix analysis of statically and kinematically indeterminate frameworks", *Int. J. Solid Struct.* **22** (1986), 409–428.

[Roth and Whiteley 1981] B. Roth and W. Whiteley, "Tensegrity frameworks"', *Trans. Am. Math. Soc.* **265** (1981), 419–446.

[Salerno 1992] G. Salerno, "How to recognize the order of infinitesimal mechanisms: A numerical approach", *Int. J. Num. Meth. Eng.* **35** (1992), 1351–1395.

[Schek 1974] H. J. Schek, "The force density method for form finding and computation of general networks", *Computer Methods in Applied Mechanics and Engineering* **3** (1974), 115–134.

[Schenk et al. 2007] M. Schenk, J. L. Herder, and S. D. Guest, "Zero stiffness tensegrity structures", *Int. J. Solids Struct.* (2007). In press.

[Skelton et al. 2001] R. E. Skelton, J. W. Helton, R. Adhikari, J. P. Pinaud, and W. Chan, *The Mechanical Systems Design Handbook: Modeling, Measurement and Control*, Chapter An introduction to the mechanics of tensegrity structures, pp. 316–386, CRC press, London, U.K., 2001.

[Skelton et al. 2002] R. E. Skelton, D. Williamson, and J. Han, "Equilibrium conditions of a class I tensegrity structure", *Spaceflight Mechanics, Advances in the Astronautical Sciences* **112**:2 (2002), 927–950.

[Snelson 1996] K. D. Snelson, "Snelson on the tensegrity invention", *Int. J. Space Struct.* **11** (1996), 43–48.

[So and Ye 2006] A. M. So and Y. Ye, "A semidefinite programming approach to tensegrity theory and realizability of graphs", pp. 766–775 in *Proceedings of the 17th Annual ACM-SIAM Symposium on Discrete Algorithms* (Miami, Florida), 2006.

[Sultan and Skelton 1998] C. Sultan and R. E. Skelton, "Tendon control deployment of tensegrity Structures", pp. 455–466 in *Proceeding of SPIE, 5th International Symposium on Smart Structures and Materials* (San Diego, California), 1998.

[Sultan et al. 2001] C. Sultan, M. Corless, and R. E. Skelton, "The prestressability problem of tensegrity strucutures. Some analytic solutions", *Int. J. Solids Struct.* **38** (2001), 5223–5252.

[Tarnai 1984] T. Tarnai, "Comments on Koiter's classification of infinitesimal mechanisms", Technical report, Hung. Inst. Build. Sci., Budapest, Hungary, 1984.

[Tibert 2002] A. G. Tibert, *Deployable tensegrity structures for space applications*, Ph.D. thesis, Royal Institute of Technology, Stockholm, Sweden, 2002.

[Tibert and Pellegrino 2003] A. G. Tibert and S. Pellegrino, "Review of form-finding methods for tensegrity structures", *Int. J. Space Struct.* **18**:4 (2003), 209–223.

[Vassart and Motro 1999] N. Vassart and R. Motro, "Multiparametered formfinding method: application to tensegrity systems", *Int. J. Space Struct.* **14**:2 (1999), 147–154.

[Vassart et al. 2000] N. Vassart, R. Laporte, and R. Motro, "Determination of mechanism's order for kinematically and statically indetermined systems", *Int. J. Solids Struct.* **37** (2000), 3807–3839.

[Williams 2003] W. O. Williams, "A primer on the mechanics of tensegrity structures", Technical report, Center for Nonlinear Analysis, Department of Mathematical Sciences, Carnegie Mellon University, Pittsburgh, Pennsylvania, 2003.

[Zhang and Ohsaki 2005] J. Y. Zhang and M. Ohsaki, "Form-finding of self-stressed structures by an extended force density method", pp. 159–166 in *Proceedings of IASS05, Int. Association for Shell and Spatial Structures* (Bucharest, Romania), 2005.

[Zhang et al. 2006] L. Zhang, B. Maurin, and R. Motro, "Form-finding of nonregular tensegrity systems", *J. Structural Engineering* **132**:9 (2006), 1435–1440.

Received May 9, 2006.

ANDREA MICHELETTI: micheletti@ing.uniroma2.it
Dipartimento di Ingegneria Civile, Università di Roma Tor Vergata, Via Politecnico 1, 00133 Rome, Italy

WILLIAM O. WILLIAMS: wow@cmu.edu
William O. Williams, Department of Mathematical Sciences, Carnegie Mellon University, Pittsburgh, PA 15213-3890, United States
http://www.math.cmu.edu/∼wow/williams